Giant optical anisotropy in an infinite-layer iron oxide $SrFeO_2$: An *ab initio* investigation

Sheng Ju[1,a)] and Tian-Yi Cai[1,2,b)]
[1]*Department of Physics and Jiangsu Key Laboratory of Thin Films, Soochow University, Suzhou, 215006, China*
[2]*Department of Physics, The University of Texas, Austin, Texas 78712, USA*

(Received 18 September 2008; accepted 18 January 2009; published online 9 February 2009)

Based on density functional theory, we study the electronic structure, magnetic structure, and linear optical response in $SrFeO_2$. For its infinite-layer structure with iron square-planar coordination, the band structure, magnetic exchange interaction, and linear dielectric function show significant anisotropic behavior. In particular, giant optical anisotropy is found. The absorption edge differs by 0.5 eV between *xx* and *zz* components, and the low frequency dielectric constant is found to be 4.26 and 5.11 for ε_{xx} and ε_{zz}, respectively. These results provide evidence of potential application of this unique structure. © *2009 American Institute of Physics*. [DOI: 10.1063/1.3079402]

Iron, one of the most abundant elements in the earth's crust, forms numerous oxides, some of which is widely used in industry as low-cost ferrite magnets.[1] They show a wide variety of electronic properties, ranging from metallic behavior to insulating one. Most of them possess oxygen octahedral and tetrahedral structures. Recently, Tsujimoto *et al.*[2] reported on the synthesis of the first ternary earth alkaline oxoferrate $SrFeO_2$, by the reduction of an easy-to-prepare, slightly oxygen-deficient perovskite $SrFeO_{3-x}$ precursor ($x=0.125$) at low temperature with CaH_2. The tetragonal $SrFeO_2$ is isotypic with $CaCuO_2$, which is the mother structure of high transition temperature superconducting materials and has the infinite-layer structure with a square-planar coordination.[2–4] As expected from crystal field theory, when the single spin down electron of $Fe^{2+}(d^6)$ occupies the degenerate orbital (d_{xz},d_{yz}), it should be subjected to orbital ordering or Jahn–Teller distortion when the temperature is lowered. However, experiment has not shown any structure instability, and $SrFeO_2$ maintains the $P4/mmm$ symmetry down to 4.2 K.[2] In the mean time, antiferromagnetic (AFM) structure with a very high Néel temperature (473 K) is found in this layered structure.[2] On the other hand, based on local density approximation plus on-site Coulomb repulsion method, two theoretical calculations were performed to explain the absence of Jahn–Teller instability as well as the origin of high Néel temperature.[5,6] In fact, for the real application, the lack of apical oxygen in $SrFeO_2$ makes its crystal structure highly anisotropic, and the high mobility of the oxygen ions would make it useful as electrodes in solid oxide fuel cell and batteries. In the mean time, the optical response will show interesting behavior.

In this letter, based on density functional theory, we reveal giant optical anisotropy in $SrFeO_2$. First, with optimized crystal structure, we compare the total energy of G-type AFM configuration [with antiparallel spin configuration between all the nearest neighboring (NN) Fe], C-type AFM (with antiparallel intralayer NN and parallel interlayer NN), A-AFM (with parallel intralayer NN and antiparallel interlayer NN), and ferromagnetic (FM) spin configurations with parallel Fe^{2+} spins. Within Heisenberg model for the spin degrees of freedom, a sizeable difference in intralayer and interlayer magnetic exchange interaction is found. Second, based on independent particle approximation and Fermi golden rule for the interband transition, we explore the linear optical response in $SrFeO_2$. The absorption edge as well as low frequency dielectric constant shows great contrast between *xx* and *zz* components. All these results are consistent with the unique anisotropic structure and provide evidence of its potential application in optoelectronics.

Our *ab initio* calculations are performed using the accurate full-potential projector augmented wave (PAW) method,[7] as implemented in the Vienna *ab initio* simulation package.[8–11] They are based on density functional theory with the generalized gradient approximation (GGA). The on-site Coulomb interaction is included in the GGA+*U* approach with effective $U=6$ eV for Fe $3d$ electrons.[12] A large plane-wave cutoff of 500 eV is used throughout, and the convergence criteria for energy is 10^{-6} eV. PAW potentials are used to describe the electron-ion interaction, with 10 valence electrons for Sr $(4s^24p^65s^2)$, 14 for Fe $(3p^63d^64s^2)$, and 6 for O $(2s^22p^4)$. Brillouin zone intergrations are performed with tetrahedron method in a $10\times10\times10$ Monkhorst–Pack *k*-point mesh centered at Γ.[13] The fully relaxed crystal structure, as shown in Fig. 1, displays a $P4/mmm$ tetragonal symmetry, with $a=b=3.990$ Å and *c*

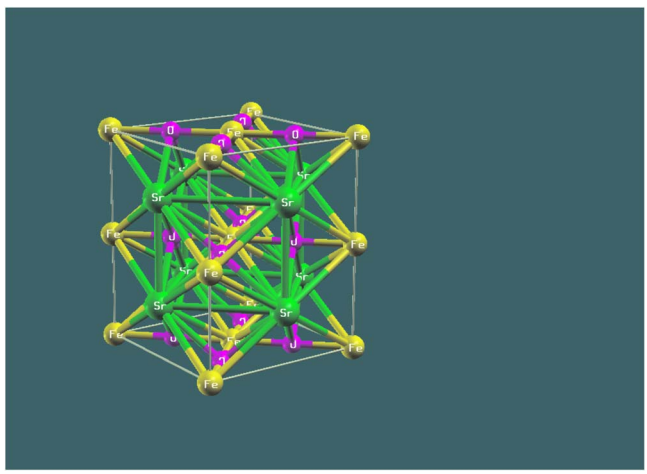

FIG. 1. (Color online) Crystal structure of $SrFeO_2$.

a)Electronic mail: jusheng@suda.edu.cn.
b)Electronic mail: tycai@physics.utexas.edu.

 © 2009 American Institute of Physics

Downloaded 23 Feb 2009 to 129.8.242.67. Redistribution subject to AIP license or copyright; see http://apl.aip.org/apl/copyright.jsp

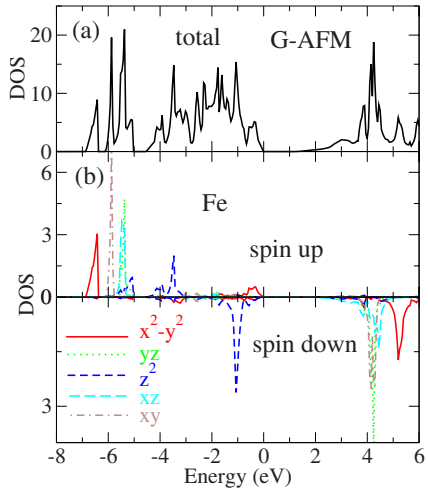

FIG. 2. (Color online) Total and partial DOS of $SrFeO_2$ with in G-type AFM spin configuration.

$=3.475$ Å, in good agreement with recent experimental data $a=b=3.985$ Å and $c=3.458$ Å.[2] A $\sqrt{2}a\times\sqrt{2}a\times 2c$ supercell is used to include all the types of spin configurations.

We first determine the magnetic ground state as well as corresponding exchange interaction constant. To do this, we compare the total energy of the four following types of magnetic ordering: G-type AFM, C-type AFM, A-type AFM, and FM. From the total energy, as listed in Table I, we find that G-type AFM is the ground state when Hubbard U is included, which is in agreement with experimental result. In the mean time, since the magnetic moments are localized at Fe^{2+} ions, the effective model for the spin degrees of freedom of $SrFeO_2$ is expected to be a Heisenberg model, with $H=-J_1\Sigma_{NN}S_iS_j-J_2\Sigma_{NN}S_iS_j-J_3\Sigma_{2NN}S_iS_j$. Here as shown in Fig. 1, we consider the interlayer nearest neighboring magnetic exchange interactions J_1, the intralayer nearest neighboring magnetic exchange interactions J_2, and the interlayer next-nearest neighboring magnetic exchange interactions J_3, with $J_1=-(1/4S^2)[E(F)-E(G)-E(A)+E(C)]$, $J_2=-(1/8S^2)\times[E(F)-E(G)+E(A)-E(C)]$, and $J_3=-(1/16S^2)[E(F)+E(G)-E(A)-E(C)]$. In the mean time, $S=2$ for Fe^{2+} ion.

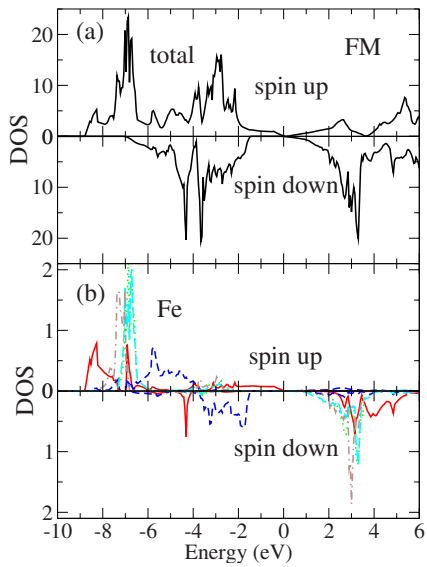

FIG. 3. (Color online) Total and partial DOS of $SrFeO_2$ with FM spin configuration.

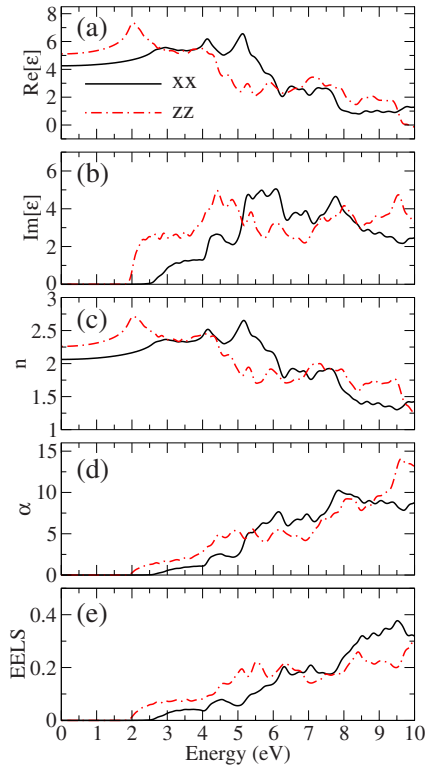

FIG. 4. (Color online) Linear optical responses of $SrFeO_2$. (a) Real part of dielectric function. (b) Imaginary part of dielectric function. (c) Refraction spectrum. (d) Absorption spectrum. (e) EELS.

From Table I, it is noted that both J_1 and J_2 are AFM, and J_3 is FM, consistent with ground G-AFM spin configuration. In the mean time, J_2 is three times larger than J_1, showing the anisotropic behavior in magnetic interactions. Since the AFM exchange interaction is proportional to $1/U$, as the decrease of U, all the exchange interaction constant decrease. Furthermore, the contrast between J_2 and J_1 increases. On the other hand, it is noted that calculations within GGA give a FM ground state, which is inconsistent with experiment. The on-site Hubbard U includes the strong correlation of d electrons of Fe. As suggested from previous *ab initio* calculations and optical measurement of $BiFeO_3$,[14,15] we focus only on the electronic and optical calculations with $U=6$ eV but the use of other U values between 3 and 6 eV do not change the giant optical anisotropy in $SrFeO_2$ revealed below.

Electronic structure is displayed in Fig. 2, where G-AFM $SrFeO_2$ is found to be an insulator with a band gap of 2 eV.

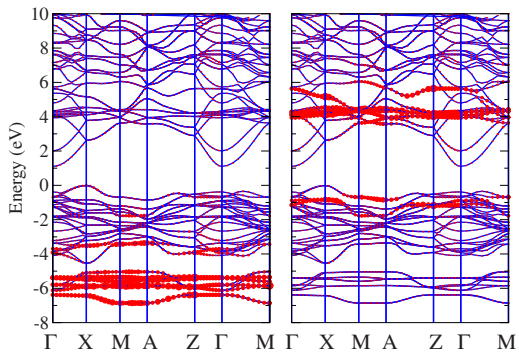

FIG. 5. (Color online) Band structure of G-type AFM $SrFeO_2$. The fatness associated with the bands is proportional to a Fe (red circles) ion.

Downloaded 23 Feb 2009 to 129.8.242.67. Redistribution subject to AIP license or copyright; see http://apl.aip.org/apl/copyright.jsp

TABLE I. Total energy (meV/f.u.) of $SrFeO_2$ with different magnetic ordering and corresponding magnetic exchange interaction constant (meV).

	G-AFM	C-AFM	A-AFM	FM	J_1	J_2	J_3
$U=6$ eV	0	15.085	79.4425	87.0525	−1.42	−4.73	0.12
$U=3$ eV	0	24.9525	147.87.425	152.497	−1.85	−8.61	0.32
$U=0$ eV	0	−2.8725	50.78	−38.805	5.77	−0.46	1.35

From the orbital selected density of states (DOS), we can find that the sixth $3d$ electron of Fe^{2+} goes to the z^2 spin down orbital. Unlike xz and yz orbital, z^2 orbital does not degenerate with any other orbital. Therefore, the electronic structure is stable and consistent with crystal $P4/mmm$ symmetry. In the mean time, the energy level of five orbitals (either the spin up channel or the spin down channel) does not agree with the simple crystal field theory. The origin for this particular orbital occupancy does not rely on the interlayer $Fe^{2+}-Fe^{2+}$ interaction or intralayer $Fe^{2+}-O^{2-}-Fe^{2+}$ interaction but on a kind of intra-atomic mechanism, where z^2 orbitals hybridize with $4s$ orbitals.[6] For the FM spin configuration (see Fig. 3), the band gap is reduced significantly. Also Fe d bands are broadened. However, the orbital occupancy does not change much, verifying the above intra-atomic mechanism. As shown in the following, such a double occupied z^2 orbitals makes the interband transition highly anisotropic.

The optical properties are calculated based on the independent-particle approximation.[16] The imaginary part of the dielectric function due to direction interband transitions is given by Fermi golden rule, i.e.,

$$\varepsilon''_{aa} = \frac{4\pi^2}{\Omega\omega^2} \sum_{i\in \mathrm{VB}, j\in \mathrm{CB}} \sum_{\mathbf{k}} w_{\mathbf{k}} |p^a_{ij}|^2 \delta(\varepsilon_{\mathbf{k}_j} - \varepsilon_{\mathbf{k}_i} - \omega), \tag{1}$$

where Ω is the unit-cell volume and ω is the photon energy. VB and CB denote the conduction and valence bands, respectively. The dipolar transition matrix elements $p^a_{ij} = \langle \mathbf{k}_j | p_a | \mathbf{k}_i \rangle$ are obtained from the self-consistent band structures within the PAW formalism. Here $|\mathbf{k}_n\rangle$ is the nth Bloch state wave function with crystal momentum $\mathbf{k}$ and a denotes the Cartesian component. The real part of the dielectric function is obtained from ε'' by a Kramers–Kronig transformation

$$\varepsilon'(\omega) = 1 + \frac{2}{\pi}\mathbf{P}\int_0^\infty d\omega \frac{\omega'\varepsilon''(\omega')}{\omega'^2 - \omega^2}, \tag{2}$$

where $\mathbf{P}$ is the principle value of the integral. In the present calculations, the δ function is approximated by a Gaussian function with $\Gamma=0.1$ eV. The dense grid of k-points $16\times16\times16$ with total irreducible 405 k-points, 20 bands per atom, and the 50 eV of the maximum energy in the integrals of real part of ε are used to guarantee the accuracy of the present optical calculations. Given the complex dielectric function $\varepsilon(\omega)=\varepsilon'(\omega)+i\varepsilon''(\omega)$, all the other linear optical properties can be calculated, e.g., linear refractive index

$$n(\omega) = \left(\frac{\sqrt{\varepsilon'^2(\omega) + \varepsilon''^2(\omega)} + \varepsilon'(\omega)}{2} \right)^{1/2}, \tag{3}$$

and the linear absorption coefficient is related to ε'' by $\alpha = \varepsilon''\omega/(nc)$, where c is the velocity of light in the vacuum. The electron energy loss spectrum (EELS) is given by $\mathrm{Im}(-1/\varepsilon)$. As shown in Fig. 4, the optical response show great contrast between two components. The absorption edge is found to be 2.5 and 2.0 eV for xx and zz component, respectively. In the mean time, the low frequency dielectric constant is 4.26 and 5.11 for ε_{xx} and ε_{zz}, respectively. These optical responses can be further understood via the band structure as shown in Fig. 5. The distribution of d orbitals is consistent with DOS shown in Fig. 2. In the mean time, z^2 orbital shows anisotropic distributed at the top of valence bands.

In summary, based on density functional theory, we have revealed anisotropic optical response in $SrFeO_2$. Together with the electronic band structure and the magnetic exchange interactions, our calculations are consistent with the unique crystal structure of $SrFeO_2$ and provide useful aspects of its potential application in optoelectronics.

S.J. thanks Professor Guang-Yu Guo of National Taiwan University for his great support. The authors gratefully acknowledge supports from the National Natural Science Foundation of China under Grant Nos. 10504023 and 10774107.

[1] J. Kohler, Angew. Chem., Int. Ed. **47**, 4470 (2008).
[2] Y. Tsujimoto, C. Tassel, N. Hayashi, T. Watanabe, H. Kageyama, K. Yoshimura, M. Takano, M. Ceretti, C. Ritter, and W. Paulus, Nature (London) **450**, 1062 (2007).
[3] C. Tassel, T. Watanabe, Y. Tsujimoto, N. Hayashi, A. Kitada, Y. Sumida, T. Yamamoto, H. Kageyama, M. Takano, and K. Yoshimura, J. Am. Chem. Soc. **130**, 3764 (2008).
[4] S. Inoue, M. Kawai, Y. Shimakawa, M. Mizumaki, N. Kawamura, T. Watanabe, Y. Tsujimoto, H. Kageyama, and K. Yoshimura, Appl. Phys. Lett. **92**, 161911 (2008).
[5] H. J. Xiang, S. H. Wei, and W. H. Whangbo, Phys. Rev. Lett. **100**, 167207 (2008).
[6] J. M. Pruneda, J. Iniguez, E. Canadell, H. Kageyama, and M. Takano, Phys. Rev. B **78**, 115101 (2008).
[7] P. E. Blochl, Phys. Rev. B **50**, 17953 (1994).
[8] G. Kresse and J. Hafner, Phys. Rev. B **47**, 558 (1993).
[9] G. Kresse and J. Hafner, Phys. Rev. B **49**, 14251 (1994).
[10] G. Kresse and J. Furthmuller, Comput. Mater. Sci. **6**, 15 (1996).
[11] G. Kresse and D. Joubert, Phys. Rev. B **59**, 1758 (1999).
[12] S. L. Dudarev, G. A. Botton, S. Y. Savrasov, C. J. Humphreys, and A. P. Sutton, Phys. Rev. B **57**, 1505 (1998).
[13] P. E. Blochl, O. Jepsen, and O. K. Andersen, Phys. Rev. B **49**, 16223 (1994).
[14] J. F. Ihlefeld, N. J. Podraza, Z. K. Liu, R. C. Rai, X. Xu, T. Heeg, Y. B. Chen, J. Li, R. W. Collins, J. L. Musfeldt, X. Q. Pan, J. Schubert, R. Ramesh, and D. G. Schlom, Appl. Phys. Lett. **92**, 142908 (2008).
[15] Our GGA+U calculations on AFM $BiFeO_3$ indicate that band gap and linear dielectric function with effective $U=6$ eV agrees with experimental data in Ref. 14.
[16] G. Y. Guo, K. C. Chu, D. S. Wang, and C. G. Duan, Phys. Rev. B **69**, 205416 (2004).

Downloaded 23 Feb 2009 to 129.8.242.67. Redistribution subject to AIP license or copyright; see http://apl.aip.org/apl/copyright.jsp